

What Is Your Diagnosis?

In cooperation with

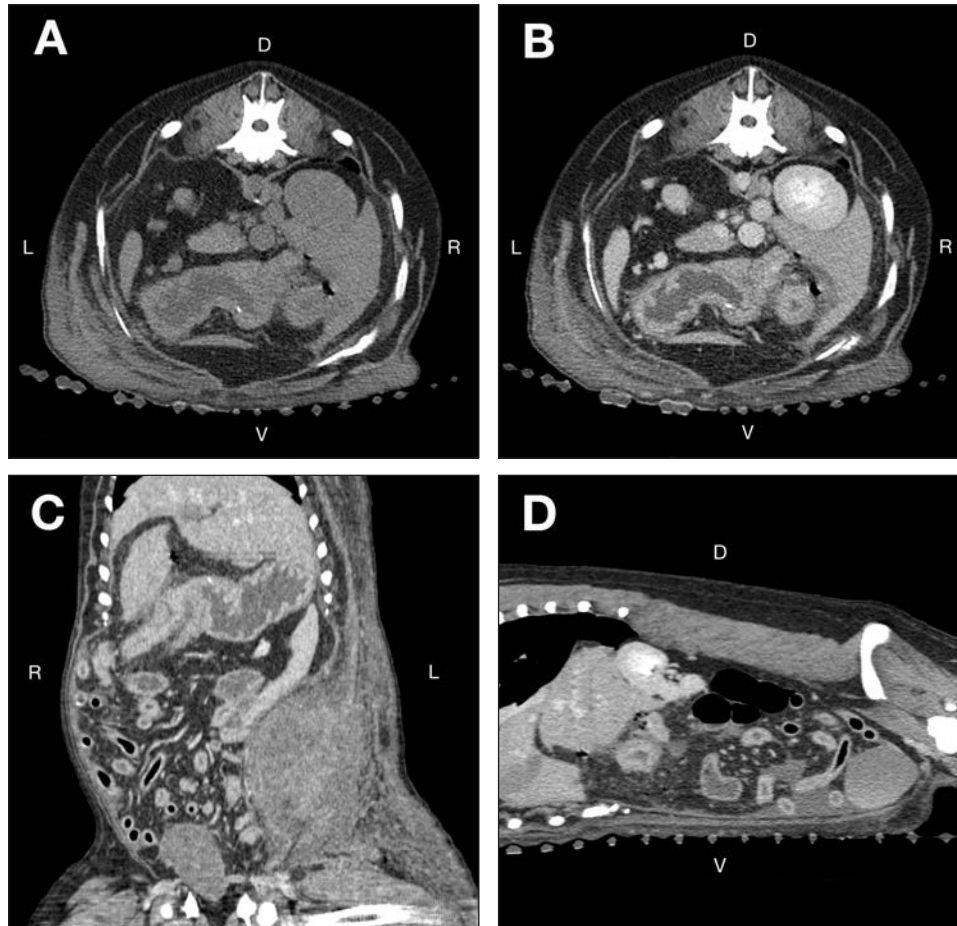


Figure 1—Transverse precontrast (A) and postcontrast (B) abdominal CT images at the level of the right kidney and reformatted postcontrast abdominal CT images in a dorsal plane through the ventral portion of the abdomen at the level of the body of the stomach (C) and in a right parasagittal plane through the right kidney (D) of a 9-year-old Golden Retriever evaluated because of lethargy, inappetence of 3 days' duration, and a body wall mass on the left side of the caudal aspect of the abdomen. Soft tissue settings were used for all images (window width, 400 Hounsfield units; window level, 40 Hounsfield units). D = Dorsal. L = Left. R = Right. V = Ventral.

History

A 9-year-old castrated male Golden Retriever was evaluated because of lethargy, inappetence of 3 days' duration, and a body wall mass on the left side of the caudal aspect of the abdomen. On physical examination, the dog was quiet, alert, and responsive. The dog had a high body temperature (39.7°C [103.4°F]) and tachycardia (210 beats/min); the dog was panting and was estimated to be 5% dehydrated. Abdominal palpation revealed that the mass was approximately 10 cm in diameter and was located within the subcutaneous tissues. The mass was firm, warm, and red with severe superficial bruising; signs of pain, however, were not elicited when the mass was palpated.

Thoracic radiography revealed a small cardiac silhouette (vertebral heart score, 8.5 vertebral lengths; reference range, 8.7 to 10.7 vertebral lengths) and faint pulmonary vasculature; these findings were consistent with hypovolemia. On abdominal ultrasonography, the mass within the subcutaneous tissues appeared moderately well demarcated and echogenically complex (hypo-, hyper-, and anechoic). The affected subcutaneous tissues and adjacent abdominal wall were hyperechoic and contained anechoic striations throughout. Differential diagnoses for the mass included neoplasia, granuloma, or abscess with adjacent cellulitis, edema, or hemorrhage. The dog's condition slowly deteriorated during the next 10 hours. For further evaluation, the dog underwent abdominal CT (Figure 1).

Determine whether additional imaging studies are required, or make your diagnosis from Figure 1—then turn the page →

This report was submitted by Elizabeth Huynh, DVM; Wm Tod Drost, DVM; and Alexis McMurray, DVM, MS; from the Veterinary Medical Center, College of Veterinary Medicine, The Ohio State University, Columbus, OH 43210. Dr. Huynh's present address is Animal Specialty and Emergency Center, 1535 S Sepulveda Blvd, Los Angeles, CA 90025. Dr. McMurray's present address is ACCES A BluePearl Veterinary Partners Hospital, 11536 Lake City Way NE, Seattle, WA 98125. Address correspondence to Dr. Huynh (huynh.elizabeth1@gmail.com).

Diagnostic Imaging Findings and Interpretation

On CT evaluation, small foci of gas are evident throughout the peritoneum with the largest amount along the nondependent aspect of the ventral portion of the abdomen (Figure 2). A mild to moderate amount of peritoneal fluid is evident along the dependent aspect of the abdomen. A 14.6 × 11.4 × 8.6-cm, well-demarcated, smoothly marginated, peripherally contrast-enhancing

heterogenous soft tissue- to fluid-attenuating mass is evident in the caudal aspect of the abdomen on the left side. Differentiation between the mass and the external abdominal body wall musculature is not possible. The entirety of the abdominal subcutaneous tissues on the left side is thickened with numerous wispy to curvilinear soft tissue-attenuating striations throughout. The height of the right limb of the pancreas is 1.6 cm (reference value,¹ 1.2 cm), and its margins are poorly defined. In the right cranial portion of the abdomen,

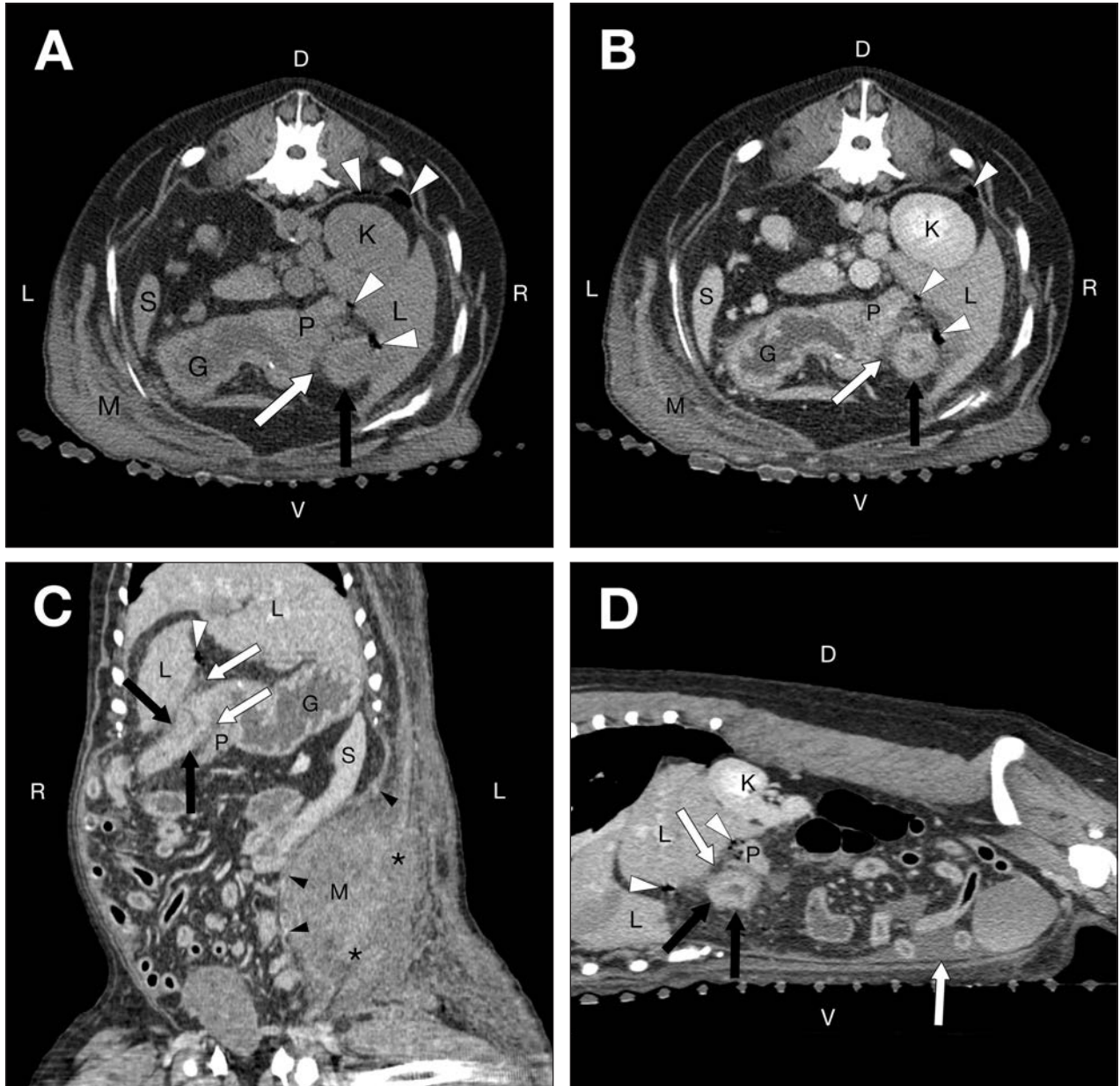


Figure 2—Same abdominal CT images as in Figure 1. On the precontrast (A) and postcontrast (B) transverse images, note the multiple small gas bubbles (arrowheads) adjacent to the thickened duodenum (black arrow), peritoneal fluid (white arrow), and a subjectively large pancreas. A portion of the body wall mass can be seen. The thickened duodenum is more conspicuous after contrast medium administration. On the reformatted postcontrast, dorsal plane (C) and reformatted postcontrast, right parasagittal plane (D) images note multiple hypoattenuating small gas bubbles (white arrowheads) adjacent and cranial to the thickened duodenum (black arrows) and adjacent and caudal to the liver. Most of the peritoneal fluid (white arrows) is observed in the dependent (ventral) aspect of the abdomen, and scant amounts of peritoneal fluid are found in the spaces between the liver and duodenum and the duodenum and pancreas. The mass causes medial deviation of the peritoneum and is peripherally contrast enhancing (black arrowheads). Differentiation between the mass and the abdominal body wall musculature is not possible (asterisks). G = Stomach. K = Right kidney. L = Liver. M = Body wall mass. P = Pancreas. S = Spleen. See Figure 1 for remainder of key.

a section of duodenal wall is thickened and measured approximately 1 cm, whereas the more aboral duodenal wall measured 0.6 cm thick (reference value for ultrasonographic duodenal wall thickness,² approx 0.53 cm). Numerous, small, punctate, mineral to metal attenuations are seen within the gastric lumen.

On the basis of CT findings, diagnoses were pneumoperitoneum, peritonitis, pancreatitis, duodenitis, and a body wall mass on the left side of the caudal aspect of the abdomen. Given the duodenal thickening with adjacent gas bubbles and peritoneal fluid, an intestinal perforation was the most likely cause of the deteriorating clinical signs. A differential diagnosis for the body wall mass was neoplasia with concurrent necrosis; less likely differential diagnoses were an abscess or granuloma with extensive cellulitis, hemorrhage, and edema. The intestinal perforation was not thought to be related to the abdominal mass.

Treatment and Outcome

Exploratory celiotomy was performed; all abdominal serosal surfaces were inflamed, with extensive petechial hemorrhages. A 2-cm perforation in the descending duodenum on the mesenteric border was found, which corresponded to the location of the thickened duodenum seen on CT evaluation. Two small circular erosions within focal, thin-walled areas of the duodenum were found on either side of the duodenal papilla along the antimesenteric border. Because of the location of the perforations and erosions, the affected intestine was not amenable to resection and anastomosis. The dog was euthanized while under general anesthesia. The mass on the left external abdominal oblique muscles and overlying subcutaneous tissues was partially resected and submitted for histologic evaluation; the duodenum was not submitted. The body wall mass had pyogranulomatous inflammation with abundant granulation tissue, hemorrhage, edema, and fibrin. No evidence of neoplasia, fungal organisms, or bacterial organisms was observed, but the pattern of inflammation of the mass suggested a fungal or bacterial organism as the inciting cause.

Comments

Gastrointestinal perforation may lead to life-threatening consequences that require immediate intervention, so early detection is important. In the dog of the present report, the timing of onset of the intestinal perforation was unknown. The progression of clinical signs along with multimodal diagnostic imaging findings raised the suspicion of gastrointestinal perforation

and aided in the localization of the defect for surgical planning to confirm gastrointestinal perforation.

Computed tomography provided detailed information, including changes in intestinal wall thickness and the presence of peritoneal gas or fluid that indicated gastrointestinal perforation. Computed tomography offers the most accurate depiction of the abdominal changes suggestive of gastrointestinal perforation in people.³ Computed tomography provides spatial and contrast resolution of the abdominal anatomy, which are often obscured by overlying structures with other imaging modalities.⁴ In people, the use of abdominal CT provides approximately 86% accuracy in determining the location of gastrointestinal perforation through the identification of extraluminal air bubbles, segmental intestinal wall thickening, and focal intestinal wall defects.³

Other imaging modalities that can be used to detect pneumoperitoneum include horizontal-beam radiography and abdominal ultrasonography.^{5,6} For horizontal-beam radiography, the animal is positioned in left lateral recumbency (ventrodorsal projection) for greater accuracy in detecting pneumoperitoneum.⁵ Typical ultrasonographic findings of gastrointestinal perforation include peritoneal fluid, gastrointestinal wall thickening, peritoneal gas, pancreatic changes, and mineralization of the gastric wall.⁷ Ultrasonographically, small volumes of peritoneal gas may appear as focal reverberation artifacts adjacent to the nondependent portion of the parietal peritoneum.⁶

On the basis of the history, physical examination findings, and CT findings, gastrointestinal perforation was suspected in the dog of the present report. Additionally, CT provided information on the involvement and extent of the subcutaneous mass into the abdominal wall.

1. Caceres AV. Pancreas. In: Schwarz T, Saunders J, eds. *Veterinary computed tomography*. Oxford, England: Wiley-Blackwell, 2011;315–324.
2. Riedesel EA. The small bowel. In: Thrall DE, ed. *Textbook of veterinary diagnostic radiology*. 6th ed. Philadelphia: WB Saunders Co, 2012;789–811.
3. Hainaux B, Agneessens E, Bertinotti R, et al. Accuracy of MDCT in predicting site of gastrointestinal tract perforation. *AJR Am J Roentgenol* 2006;187:1179–1183.
4. Hoey S, Drees R, Hetzel S. Evaluation of the gastrointestinal tract in dogs using computed tomography. *Vet Radiol Ultrasound* 2013;54:25–30.
5. Marolf A, Blaik M, Ackerman N, et al. Comparison of computed radiography and conventional radiography in detection of small volume pneumoperitoneum. *Vet Radiol Ultrasound* 2008;49:227–232.
6. Ferrell EA, Graham JP. Ultrasound corner: diagnosis of pneumoperitoneum. *Vet Radiol Ultrasound* 2003;44:307–308.
7. Boysen SR, Tidwell AS, Penninck DG. Ultrasonographic findings in dogs and cats with gastrointestinal perforation. *Vet Radiol Ultrasound* 2003;44:556–564.